Fuzzy Tracking and Control Algorithm for an SSVEP-Based BCI System

Yeou-Jiunn Chen [1], Shih-Chung Chen [1], Ilham A. E. Zaeni [1] and Chung-Min Wu [2,*]

[1] Department of Electrical Engineering, Southern Taiwan University of Science and Technology, Tainan 710, Taiwan; chenyj@stust.edu.tw (Y.-J.C.); chung@stust.edu.tw (S.-C.C.); ilhamaez81@gmail.com (I.A.E.Z.)

[2] Department of Computer and Communication, Kun-Shan University, Tainan 710, Taiwan

[*] Correspondence: cmwu@mail.ksu.edu.tw; Tel.: +886-6-2050521 (ext. 2503)

Abstract: Subjects with amyotrophic lateral sclerosis (ALS) consistently experience decreasing quality of life because of this distinctive disease. Thus, a practical brain-computer interface (BCI) application can effectively help subjects with ALS to participate in communication or entertainment. In this study, a fuzzy tracking and control algorithm is proposed for developing a BCI remote control system. To represent the characteristics of the measured electroencephalography (EEG) signals after visual stimulation, a fast Fourier transform is applied to extract the EEG features. A self-developed fuzzy tracking algorithm quickly traces the changes of EEG signals. The accuracy and stability of a BCI system can be greatly improved by using a fuzzy control algorithm. Fifteen subjects were asked to attend a performance test of this BCI system. The canonical correlation analysis (CCA) was adopted to compare the proposed approach, and the average recognition rates are 96.97% and 94.49% for proposed approach and CCA, respectively. The experimental results showed that the proposed approach is preferable to CCA. Overall, the proposed fuzzy tracking and control algorithm applied in the BCI system can profoundly help subjects with ALS to control air swimmer drone vehicles for entertainment purposes.

Keywords: brain-computer interface; steady-state visual evoked potentials; fuzzy logic; CCA

1. Introduction

Amyotrophic lateral sclerosis (ALS) attacks the motor neurons. Numerous ALS patients around the world report that ALS seriously reduces the quality of their lives. ALS critically reduces their motor abilities; they experience difficulties in performing daily activities, such as participating in entertainment activities. Therefore, in recent years, an extensive range of high technology assistive devices have been developed to fulfill the needs of these individuals. These assistive devices can help these patients perform daily activities such as eating, communicating, and moving from place to place. Although assistance in performing daily activities is essential, the psychological effects of nonessential patient activities such as entertainment should also be considered. Therefore, the development of a brain-computer interface (BCI) application for entertainment is worthwhile for subjects with ALS.

A BCI is used to give commands to a computer or other device through electroencephalography (EEG) measurements taken from sensors on a human scalp. A BCI is not necessary for the implementation of any sensor into the brain, so it can easily be applied to subjects with motor neuron disease [1]. This technology can effectively and easily help subjects with ALS to communicate with the outside world [2]. A BCI can be developed using P300 waves, motor imagery, event-related potential, visual evoked potential, and steady-state visual evoked potential (SSVEP) [3–9]. A P300-based BCI is operated by asking the user to select a row and a column from a command matrix [4]. BCI applications

can integrate several methods, such as P300 and SSVEP [5,6]. A suitable BCI for subjects with ALS may enable those subjects to operate various devices, including entertainment devices.

SSVEP technology has been utilized in BCI applications by using visual stimuli to induce human brain waves and trigger brain potentials [3]. Several boxes with different flickering frequencies can be used as stimuli for SSVEP applications [7]. Other researchers have used several boxes that flickered at the same frequency but with different phases as stimuli for an SSVEP application [8]. The light source that was used as a stimulus also varied. Some research has used liquid-crystal display (LCD) monitors as stimuli, and other research has used LEDs as stimuli. A SSVEP-based BCI is one of the easiest interfaces to implement for subjects with ALS.

Several studies have been proposed to develop BCI applications for entertainment. A BCI application was designed to help people with severe disabilities play tennis games on a computer [10]. The use of consumer-grade equipment rather than research lab-grade equipment for BCI gaming applications can improve public awareness of BCI technology. SSVEP technology can be adopted to provide excellent control when applied in a tactical video game [11]. Another SSVEP-based BCI application was used to control an avatar in a maze game. Four commands triggered by responses to stimuli, namely up, down, left, and right, controlled the movement of an avatar in a maze [12]. Phase-tagging SSVEP has been implemented to control spacecraft movement to avoid obstacles. Two stimuli with 180° phase differences and frequencies in the 3–5 Hz range were used to produce inputs for controlling left or right movements [13].

In general, most fuzzy recognition algorithms contain three processes: fuzzification, inference rules, and defuzzification. In fuzzy recognition algorithms, fuzzy sets and fuzzy logic are used for heuristic quantification of the meanings of linguistic variables, linguistic values, and linguistic rules that are specified by experts. The concept of a fuzzy set can be introduced by first defining a "membership function." Fuzzy sets are used to quantify the information in the rule-base, and the inference mechanism operates on fuzzy sets to produce fuzzy sets; hence, the fuzzification process converts numeric inputs into fuzzy sets. The inference mechanism has two basic tasks: (1) determining the extent to which each rule is relevant to the current situation, as characterized by the inputs; and (2) drawing conclusions by using the current inputs and the information in the rule-base. The defuzzification process generates the output of fuzzy inference, which is a crisp value for a controlled system. The fuzzy recognition algorithm is simple and fast; thus, it is suitable for a real-time SSVEP-based BCI system.

EEG signals are small, varying, and complex, so accurately recognizing EEG features is extremely difficult. Fuzzy sets can easily be installed in single-chip microprocessors. Single-chip fuzzy inference systems have been widely used in numerous applications, especially for real-time systems [14]. Lou and Loparo combined wavelet methods and fuzzy algorithms to implement a bearing fault detection system [15]. An adaptive neurofuzzy inference system (ANFIS) was used to classify breast mass [16]. Güler and Übeyli used ANFIS to detect electrocardiographic (ECG) changes in patients with partial epilepsy [17] and classify EEG signals [18]. However, an ANFIS must collect a training database for parameter estimation of a neural network. The performance of an ANFIS would be degraded when its user's EEG data is not collected. Achieving real-time recognition for a BCI-based application is essential, as is adapting the system so that it can quickly fit a new user.

In this study, a fuzzy tracking and control algorithm is proposed for helping subjects with ALS use a BCI remote control system. For accurate representation of EEG signal characteristics, a fast Fourier transform (FFT) was applied to extract the power spectrum, which involves the features for recognition. To quickly track the changes of EEG signal characteristics, a fuzzy tracking algorithm was developed. To improve the accuracy and stability of this BCI system, a fuzzy control algorithm is proposed. To help subjects with ALS operate remote-controlled devices, a BCI-based air swimmer drone vehicle was developed.

The remainder of this paper is organized as follows. Section 2 describes the fuzzy tracking and control algorithms and discusses visual stimulation and signal acquisition. Section 3 presents the results

of a series of experiments and evaluates the performance of our approach. Finally, conclusions are drawn in Section 4, and possible improvements for the future development of this work are discussed.

2. Methods

A block diagram of the proposed system is shown in Figure 1. First, the subject sits on a chair in front of an LCD screen and focuses on the flickering boxes that appear on the screen. Second, the EEG signals are acquired using electrodes placed on the occipital region of the subject's head. Third, the preprocessing step of the EEG signal removes noise from the signal. Fourth, the features of the EEG signal are extracted by using FFT to derive the energy of each stimulus frequency. Finally, a fuzzy tracking and control algorithm is applied to recognize the appropriate response, which is used to control the air swimmer drone vehicle. A detailed description is provided in the following subsections.
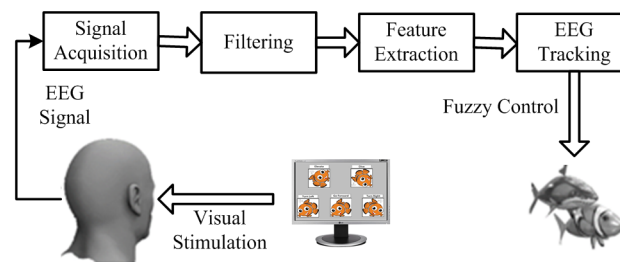

Figure 1. Brain-computer interface (BCI) remote control system architecture.

2.1. Visual Stimulation and Feature Extraction

To elicit SSVEP, an LCD monitor displayed visual stimulation in the form of flickering boxes, and the BCI layout of the visual stimulation is shown in Figure 2. The subject was asked to sit at a distance of 55 cm from the monitor, measured from the subject's nasion to the BCI screen. For an LCD monitor, the refresh rate was typically 60 Hz; thus, the flickering boxes could flicker in a limited range of frequencies [19]. With such a refresh rate, it was possible to simulate different frequencies by displaying appropriate numbers of frames. Rendering an order of frames can generate a flickering box with a desired frequency. According to clinical experience, a visual stimulation ranging from 15–25 Hz can easily evoke an epileptic syndrome. Therefore, the selected frequencies were lower than 10 Hz in this study. The five orders of frames and corresponding frequencies that were used as stimuli are listed in Table 1. For an order of frames, the numbers 1 and 0 were used to represent a frame with an image and a black box, respectively. The duty cycle was therefore not always equal to 0.5, as the number of frames in one period is an odd number.
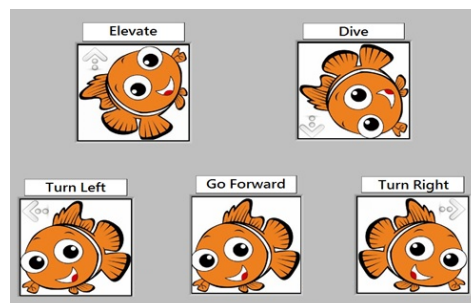

Figure 2. The BCI layout for an air swimmer drone vehicle.

Table 1. Frequencies for a screen with a refresh rate of 60 Hz.

The Number of Frames	Period (ms)	Frequency (Hz)	Simulated Signal
6	100.00	10.00	111000
7	116.67	8.57	1111000
8	133.33	7.50	11110000
9	150.00	6.67	111110000
10	166.67	6.00	1111100000

When the visual stimulation elicited signals in the visual cortex of the brain, EEG signals were simultaneously read from the occipital region of the subject's head by using a NuAmps EEG amplifier supplied by the Neuroscan Company. The EEG signals were then acquired from the Oz channel with reference and ground electrodes placed at A1 and A2. When an EEG signal x was acquired, a power spectrum sequence X with N frames was estimated by using the Hamming window and FFT. For the kth frame, $X(k)$, a triangular window centered at f_c Hz was then applied to calculate the band energy for each stimulus with a flicker frequency of f_c Hz; it was treated as an input feature for the fuzzy tracking and control algorithm.

2.2. Fuzzy Tracking and Control Algorithm

The block diagram of the fuzzy tracking and control algorithm is shown in Figure 3. For the kth frame, $X(k)$, the prediction error e_k of a fuzzy algorithm was estimated as

$$e_k = X(k) - \tau_{k\text{-}1}, \tag{1}$$

where $\tau_{k\text{-}1}$ is the threshold at the k-1 frame. The initial threshold value, τ_0, is a predefined value; it can be estimated by using the average power energy of first M-frames.
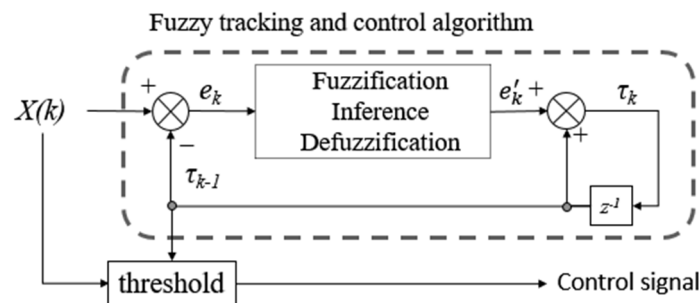

Figure 3. Structure of fuzzy tracking and control algorithm. The variable z^{-1} is a unit delay for the next step.

Because the Mamdani inference model [20] combines the sets and rules for fast and simple calculation, it was selected with linguistic rules for defining the relation between the input and the output. The fuzzy set A (Figure 4) and B (Figure 5) were used in the fuzzification and defuzzification processes. The input range of fuzzifier and the output range of defuzzifier were from $-R_f$ to R_f and $-R_d$ to R_d, respectively. Considering the performance and stability of a recognition algorithm in a microprocessor, the number of fuzzy sets was five [21]. The linguistic parameters of these five fuzzy sets were negative large (LN), negative small (SN), zero (ZE), positive small (SP), and positive large (LP). According to the fuzzy set calculations, the fuzzy inference rules were as follows.

If $e_k \in LN$ then $\widetilde{e}_k \in LN$,
if $e_k \in SN$ then $\widetilde{e}_k \in SN$,
if $e_k \in ZE$ then $\widetilde{e}_k \in ZE$,

if $e_k \in SP$ then $\widetilde{e}_k \in SP$,

and

if $e_k \in LP$ then $\widetilde{e}_k \in LP$,

where e_k and $\widetilde{e}_k$ are the input variable of fuzzy sets A and the output variable of fuzzy sets B, respectively.
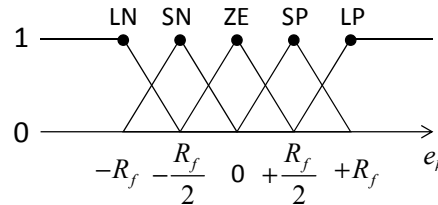

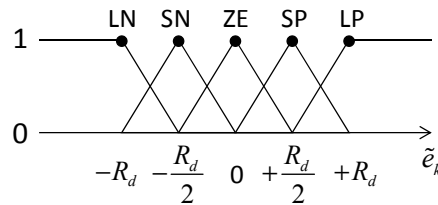**Figure 4.** Membership function of fuzzifier (fuzzy set A).

Figure 5. Membership function of defuzzifier (fuzzy set B).

A defuzzification process was then used to obtain a finite number as an output. In this study, using the center of gravity method [20], the output variable, e'_k, of fuzzy threshold could be calculated following

$$e'_k = \frac{\sum\limits_{i=1}^{n} S_i\left(e_k\right) B_i\left(\widetilde{e}_k\right)}{\sum\limits_{i=1}^{n} S_i\left(e_k\right)}, \tag{2}$$

where S_i is the membership grade of the ith premise in the inference rule, and B_i is the central value of the ith conclusion in the inference rule. The threshold value was then updated by

$$\tau_k = e'_k + \tau_{k-1}. \tag{3}$$

Finally, the output of the control signal was 1 if $X\left(k\right) \geq \tau_{k-1}$; otherwise, the output of the control signal was 0.

3. Results and Discussion

In this study, the EEG signals were recorded at a sample rate of 1k Hz and a bit resolution of 22 bits. A second-order Butterworth band-pass filter was used to remove the signals with frequencies lower than 4 Hz and higher than 60 Hz. The window size of the Hamming window was 1000 points, which was then applied to obtain a sequence of trials. Subsequently, the power energies for each visual stimulus were estimated using an FFT with 4096 points and triangular windows with 2-Hz bandwidths.

3.1. Performance of the Fuzzy Tracking and Control Algorithm

This subsection reports that fifteen healthy subjects (11 males and four females) aged between 21 and 23 were asked to participate for evaluating the fuzzy tracking and control algorithm. To collect

the training data, we developed a visual stimulation procedure comprised of five sets of stimulation sequences. Each set of stimulation sequence consisted of three stimulation frequencies that were randomly generated from the five given frequencies (6 Hz, 6.67 Hz, 10.00 Hz, 8.57 Hz, and 7.50 Hz). Each set of stimulation sequence consisting of three stimulation frequencies followed the following procedure: Each set began with a five-second countdown delay followed by a series of a ten-second visual stimulation and ten seconds of rest. Afterwards, one minute of compulsory rest time was provided for the subject after every set of stimulation sequence. The acquired EEG signals during every ten-second visual stimulation were then blocked into ten non-overlapping frames, and the duration of each frame was one second.

Because the membership functions of fuzzification and defuzzification can greatly affect the accuracy, validating the factors of membership functions such as their shapes and the ranges is crucial. For fuzzy-based approaches, the triangular function, trapezoidal function, generalized bell curve function, symmetric Gaussian function, and a two-sided version of the Gaussian are widely used [22]. Therefore, these five functions were selected as the membership functions and denoted as TriaMF, TrapMF, GbellMF, GaussMF, and Gauss2MF, respectively. The range of each membership function in fuzzification and defuzzification was examined from 5 to 50, and the results are shown in Figure 6. The results show that the recognition rates converged when the range of the membership function was greater than 20 for each membership function. When the range of the membership function did not suffice to model the features, the recognition rates were seriously degraded.
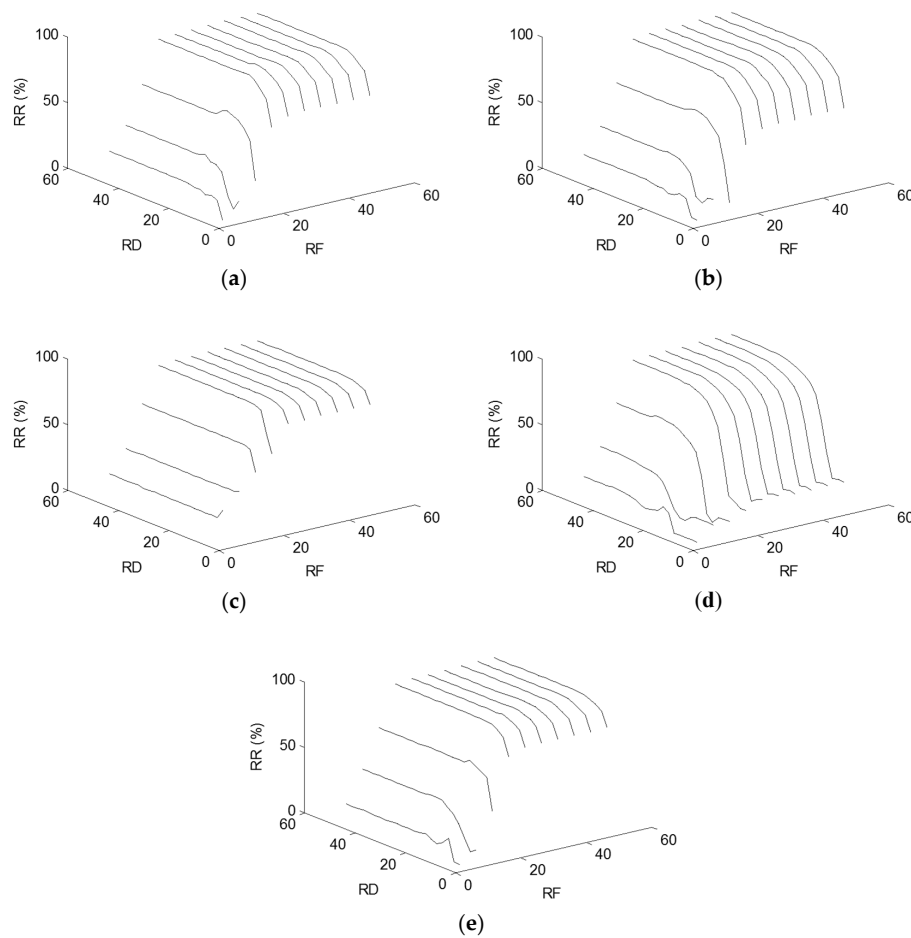

Figure 6. Recognition rates for (**a**) TriaMF; (**b**) TrapMF; (**c**) GbellMF; (**d**) GaussMF; and (**e**) Gauss2MF. RD, RF, and RR are the output range of defuzzification, the input range of fuzzification, and recognition rate, respectively.

The optimal recognition rates for the five membership functions are shown in Table 2. The results indicate that the recognition rates for different membership functions were similar. The computational time of the proposed approach was not affected by the RD or the RF, but it was greatly affected by membership functions with different levels of complexity. Since TrapMF, GbellMF, GaussMF, and Gauss2MF are second-order polynomial equations; their computational complexity are similar. However, the computational complexity of TraiMF was lower than those of the other membership functions. The difference between the optimal recognition rate (GaussMF) and the pessimal recognition rate (TriaMF) was only 0.6%; such a level of error can be ignored in numerous applications. Therefore, the TriaMF was very suitable for real-time applications and was selected in this study.

Table 2. Optimal recognition rates for different membership functions.

	TriaMF	TrapMF	GbellMF	GaussMF	Gauss2MF
Recognition rate (%)	97.02	97.56	97.64	97.69	97.51
The output range of defuzzification	20.75	27.5	27.5	34.25	27.5
The input range of fuzzification	30	40	40	50	40

3.2. Comparison with CCA

For comparison with the proposed approach, the CCA was selected as the baseline system [23]. For the mth stimulus frequency f_m, a preconstructed reference signal set was formed using a series of sin-cosine waves, which can be written as follows:

$$y_m = \begin{bmatrix} \sin(2\pi f_m t) \\ \cos(2\pi f_m t) \\ \vdots \\ \sin(2\pi H f_m t) \\ \cos(2\pi H f_m t) \end{bmatrix}, \tag{4}$$

where $t = \frac{1}{F}, \frac{2}{F}, \cdots, \frac{P}{F}$. H, P, and F are the number of harmonics, the number of points for an input signal, and the sampling rate, respectively. The number of harmonics, H, was 4 in this experiment. The experimental results of the fifteen subjects are shown in Figure 7. The recognition rates were 94.49% and 96.97% for the baseline and the fuzzy approach, respectively. The recognition rate of the proposed approach for each subject was clearly higher than that of baseline. To examine the experimental results, a Wilconxon's signed-rank test was adopted, and the two-tailed test p-value was approximately 0.002. Thus, at a signification level of 0.01, the results we obtained surely indicate that the recognition rate of the proposed approach is higher than that of CCA. Therefore, the proposed approach is an excellent solution for correctly recognizing the frequency response of the visual stimulation.
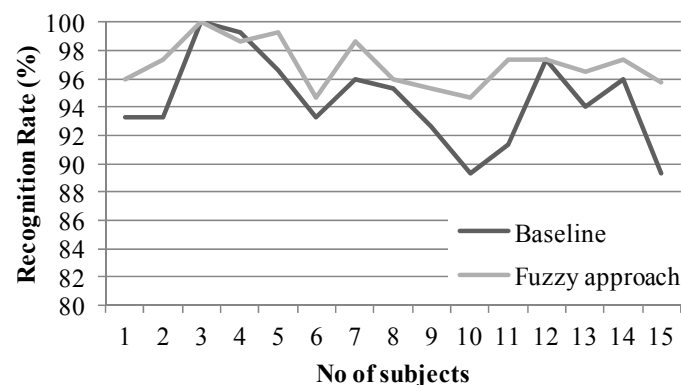

Figure 7. Experimental results for different subjects.

To analyze the effects of the visual stimulus frequency, the experimental results for different stimulus frequencies are shown in Figure 8. The results indicate that, when the stimulus frequency increased, the recognition rates were slightly degraded. To determine the cause, the normalized amplitude at the stimulus frequency, which reflects the SNR of the SSVEP, can be calculated as follows:

$$P = \frac{|FFT(x)|}{\sum\limits_{x} |FFT(x)|},\qquad(5)$$

where x is the preprocessed EEG data and $FFT(x)$ is the fast Fourier transform of x. $\sum\limits_{x} |FFT(x)|$ denotes summing over the total frequency points of the spectrum; thus, the sum of the amplitude spectrum is normalized to one [24]. The results for one subject are shown in Figure 9. The peak of the stimulus frequency can be clearly identified for that subject. However, the SNR of the peak value for a high stimulus frequency is lower than that for a low stimulus frequency. Therefore, if the stimulus frequency is increased, the performance is degraded. For the proposed approach, the adverse effects can be reduced by automatically adapting the threshold for making the decision.
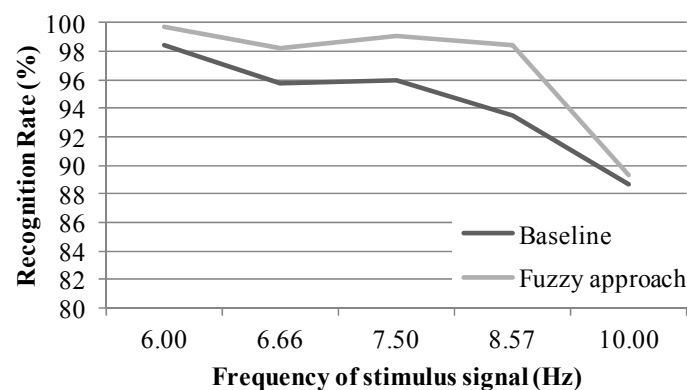

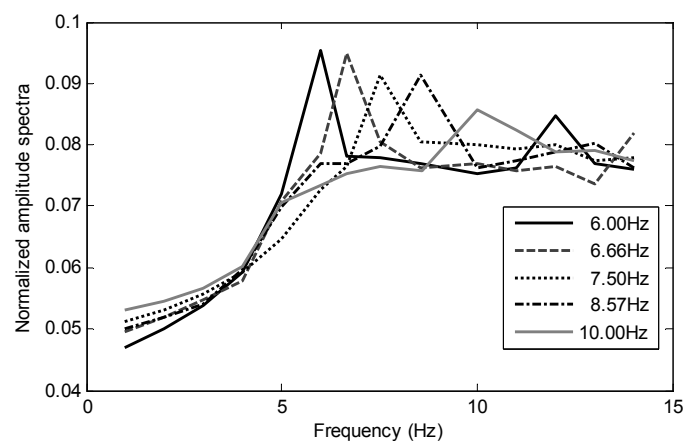**Figure 8.** Experimental results for different stimulus signals.

Figure 9. Electroencephalography (EEG) amplitude spectra corresponding to five different stimulus frequencies.

3.3. Real-Time Application

In this subsection, the fuzzy tracking and control algorithm was applied to control an air swimmer drone vehicle for subjects with ALS in entertainment. The air swimmer drone vehicle (Figure 10) could be controlled to swim through the air with incredibly smooth and life-like swimming motions. The BCI layout (Figure 2) was displayed on a 19-inch LCD monitor (4:3), and the average distance

between two centers of two adjacent flickering boxes was 13.22 cm. The range of the input triangle membership function was 40, and the range of the output triangle membership function was 28. An example of stimulus frequency response for a subject is shown in Figure 11a. In this example, a subject was asked to control the air swimmer drone vehicle with a sequence of stimulation frequencies that correspond to the commands "dive" (6 Hz), "turn left" (7.5 Hz), "go forward" (8.57 Hz), "turn right" (6.67 Hz), and "elevate" (10 Hz). The subject was requested to focus on a single command for a duration of five seconds, and EEG data of the subject was acquired every second without any time interval in between two adjacent trials. The corresponding recognition results are shown in Figure 11b. The results revealed that the proposed approach can successfully convert the SSVEP EEG signals into corresponding real-time control signals.

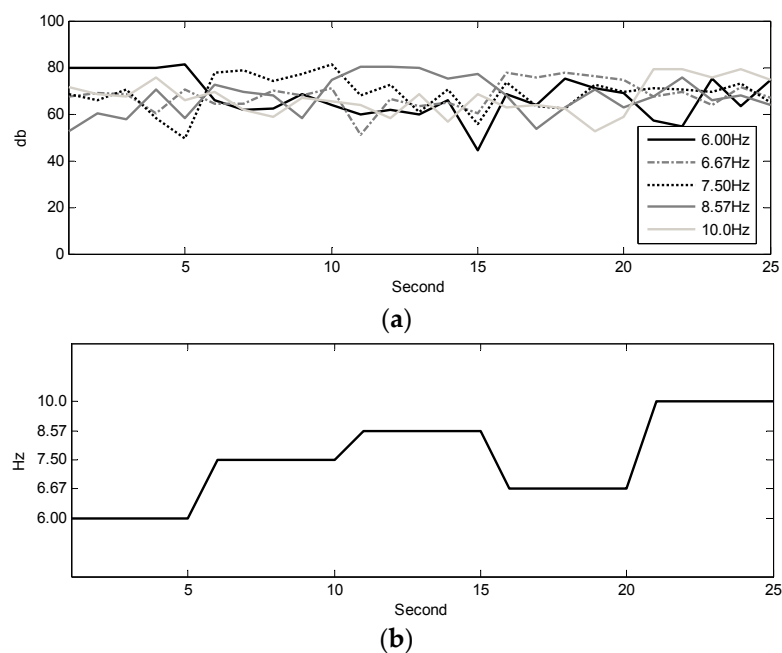**Figure 10.** User controlling an air swimmer drone vehicle through the proposed approach.

Figure 11. Steady-state visual evoked potential (SSVEP) EEG signal is converted to a control signal. (**a**) The power energy of a subject's EEG response for different stimulus frequency. (**b**) Decision results.

To evaluate the proposed approach in a real-time application, five subjects with ALS (four males and one female; age between 21 and 37) were asked to operate the air swimmer drone vehicle. For each subject, the rate of progression was measured using a revised ALS functional rating scale (ALSFRS-R) [25]. The scale of ALSFRS-R is composed of 12 items graded from 0 (complete loss of function) to 4 (normal function), with a score range between 0 (unable to perform the tested functions) and produces a score between 48 (normal function) and 0 (severe disability). The average ALSFRS-R

score of five subjects was 29.8. The participants gave informed consent, and the study was approved by Institutional Review Board of National Cheng Kung University Hospital.

Since the proposed application is to relax subjects with ALS by operating the air swimmer drone vehicle, the entertainment value is more important than the recognition rate. Thus, to quantify the entertainment value of the proposed system, the caregivers helped us to ask each subject to answer the question "Is the system interesting?" Then, each subject was asked to provide a mean opinion score (MOS) ranging from 5 (*excellent*) to 1 (*unsatisfactory*). The average MOS was 4.3. Thus, the subjects' responses indicate that the proposed system can hold the interest of subjects with ALS.

4. Conclusions

In this work, a fuzzy tracking and control algorithm was successfully developed for a single-channel SSVEP-based BCI system. The SSVEP can be successfully elicited by visual stimulation on an LCD monitor with a 60-Hz refresh rate. A fuzzy tracking algorithm was able to identify the changes of EEG signals accurately. Because the quality of EEG signals for a single-channel BCI system is low, this fuzzy tracking algorithm can improve quality by tracking a previous status. Thus, the recognition rate of the BCI system with the fuzzy tracking algorithm can be clearly improved when compared with that of a CCA baseline system. For frequencies lower than 10 Hz, the recognition curves for the CCA baseline and the proposed approach show that the recognition rates were degraded when the stimulus frequency was increased because the SNR of the peak value for a high stimulus frequency was lower than that of the low stimulus frequency. The proposed approach was successfully implemented as a BCI-based interface to control an air swimmer drone vehicle, and users were interested in this application. Fundamentally, this self-developed single-channel SSVEP-based BCI system, with its fuzzy tracking and control algorithm, can be used by general subjects without prior training. Because the computational complexity of the proposed approach is relatively simple, this approach can be implemented as a standalone embedded BCI system in the near future with numerous applications such as text input systems, neurogaming, and home appliance control. After this single-channel SSVEP-based BCI system has finished its performance tests, a more convenient and cheaper EEG acquisition device with dry electrodes could be adopted and integrated with visual stimulators and a new standalone signal processing module.

Author Contributions: Yeou-Jiunn Chen and Chung-Min Wu conceived and designed the experiments; Ilham A. E. Zaeni performed the experiments; Yeou-Jiunn Chen and Shih-Chung Chen analyzed the data; Chung-Min Wu contributed reagents, materials, and analytical tools; Yeou-Jiunn Chen, Shih-Chung Chen, Ilham A. E. Zaeni, and Chung-Min Wu wrote the paper.

Conflicts of Interest: The authors declare that there is no conflict.

References

1. Carabalona, R.; Grossi, F.; Tessadri, A.; Castiglioni, P.; Caracciolo, A.; de Munari, I. Light on! Real world evaluation of a P300-based brain–computer interface (BCI) for environment control in a smart home. *Ergonomics* **2012**, *55*, 552–563. [CrossRef] [PubMed]
2. McFarland, D.J.; Wolpaw, J.R. Brain-computer interfaces for communication and control. *Commun. ACM* **2011**, *54*, 60–66. [CrossRef] [PubMed]
3. Cecotti, H. Spelling with non-invasive Brain–Computer Interfaces–Current and future trends. *J. Physiol.-Paris* **2011**, *105*, 106–114. [CrossRef] [PubMed]
4. Farwell, L.A.; Donchin, E. Talking off the top of your head: Toward a mental prosthesis utilizing event-related brain potentials. *Electroencephalogr. Clin. Neurophysiol.* **1988**, *70*, 510–523. [CrossRef]
5. Xu, M.; Qi, H.; Wan, B.; Yin, T.; Liu, Z.; Ming, D. A hybrid BCI speller paradigm combining P300 potential and the SSVEP blocking feature. *J. Neural Eng.* **2013**, *10*, 026001. [CrossRef] [PubMed]

6. Erwei, Y.; Zongtan, Z.; Jun, J.; Fanglin, C.; Yadong, L.; Dewen, H. A novel hybrid BCI speller based on the incorporation of SSVEP into the P300 paradigm. *J. Neural Eng.* **2013**, *10*, 026012. [CrossRef]

7. Azom, M.A.; Rana, M.M.; Ahmad, M. Design and implementation of a user independent SSVEP based brain-computer interface with high transfer rates. In Proceedings of the 2013 International Conference on Informatics, Electronics & Vision (ICIEV), Dhaka, Bangladesh, 17–18 May 2013; pp. 1–6.

8. Yeh, C.L.; Lee, P.L.; Chen, W.M.; Chang, C.Y.; Wu, Y.T.; Lan, G.Y. Improvement of classification accuracy in a phase-tagged steady-state visual evoked potential-based brain computer interface using multiclass support vector machine. *BioMed. Eng. OnLine* **2013**, *12*, 46. [CrossRef] [PubMed]

9. Chen, Y.J.; See, A.R.A.; Chen, C.C. SSVEP-based BCI classification using power cepstrum analysis. *IEEE Electron. Lett.* **2014**, *50*, 735–737. [CrossRef]

10. Lopetegui, E.; Garcia Zapirain, B.; Mendez, A. Tennis computer game with brain control using EEG signals. In Proceedings of the 2011 16th International Conference on Computer Games (CGAMES), Louisville, KY, USA, 27-30 July 2011; pp. 228–234.

11. Van Vliet, M.; Robben, A.; Chumerin, N.; Manyakov, N.V.; Combaz, A.; Van Hulle, M.M. Designing a brain-computer interface controlled video-game using consumer grade EEG hardware. In Proceedings of the Biosignals and Biorobotics Conference (BRC), 2012 ISSNIP, Manaus, Brazil, 9–11 January 2012; pp. 1–6.

12. Chumerin, N.; Manyakov, N.V.; van Vliet, M.; Robben, R.; Combaz, A.; Van Hulle, M. Steady-State Visual Evoked Potential-Based Computer Gaming on a Consumer-Grade EEG Device. *IEEE Trans. Comput. Intell. AI Games* **2013**, *5*, 100–110. [CrossRef]

13. Parafita, R.; Pires, G.; Nunes, U.; Castelo-Branco, M. A spacecraft game controlled with a brain-computer interface using SSVEP with phase tagging. In Proceedings of the 2013 IEEE 2nd International Conference on Serious Games and Applications for Health (SeGAH), Vilamoura, Portugal, 2–3 May 2013; pp. 1–6.

14. Wu, C.M.; Luo, C.H. Morse code recognition system with fuzzy algorithm for disabled persons. *J. Med. Eng. Tech.* **2002**, *26*, 202–207. [CrossRef] [PubMed]

15. Lou, X.; Loparo, K.A. Bearing fault diagnosis based on wavelet transform and fuzzy inference. *Mech. Syst. Signal Process.* **2004**, *18*, 1077–1095. [CrossRef]

16. Gorgel, P.; Sertbas, A.; Ucan, O.N. A fuzzy inference system combined with wavelet transform for breast mass classification. In Proceedings of the 2012 35th International Conference on Telecommunications and Signal Processing (TSP), Prague, Czech, 3–4 July 2012; pp. 644–647.

17. Güler, İ.; Übeyli, E.D. Application of adaptive neuro-fuzzy inference system for detection of electrocardiographic changes in patients with partial epilepsy using feature extraction. *Expert Syst. Appl.* **2004**, *27*, 323–330. [CrossRef]

18. Güler, İ.; Übeyli, E.D. Adaptive neuro-fuzzy inference system for classification of EEG signals using wavelet coefficients. *J. Neurosci. Method.* **2005**, *148*, 113–121. [CrossRef] [PubMed]

19. Cecotti, H.; Volosyak, I.; Graser, A. Reliable visual stimuli on LCD screens for SSVEP based BCI. In Proceedings of the The 2010 European Signal Processing Conference (EUSIPCO-2010), Aalborg, Denmark, 23–27 August 2010; pp. 919–923.

20. Mamdani, E.H. Application of fuzzy logic to approximate reasoning using linguistic synthesis. *IEEE Trans. Comput.* **1977**, *C-26*, 1182–1191. [CrossRef]

21. Wu, C.M.; Luo, C.H.; Lin, S.W. Mouth-controlled text input device with sliding fuzzy algorithm for individuals with severe disabilities. *Biomed. Eng. Appl. Basis Commun.* **2010**, *22*, 223–237. [CrossRef]

22. Passino, K.M.; Yurkovich, S. *Fuzzy Control*; Addison Wesley Longman: Menlo Park, CA, USA, 1995.

23. Zhang, Y.; Zhou, G.; Jin, J.; Wang, X.; Cichocki, A. Frequency Recognition in SSVEP-based BCI using Multiset Canonical Correlation Analysis. *Int. J. Neural Syst.* **2014**, *24*, 1450013. [CrossRef] [PubMed]

24. Wang, Y.; Wang, R.; Gao, X.; Hong, B.; Gao, S. A practical VEP-based brain-computer interface. *IEEE Trans. Neural Syst. Rehabil. Eng.* **2006**, *14*, 234–239. [CrossRef] [PubMed]

25. Castrillo-Viguera, C.; Grasso, D.L.; Simpson, E.; Shefner, J.; Cudkowicz, M.E. Clinical significance in the change of decline in ALSFRS-R. *Amyotroph. Lateral Scler.* **2010**, *11*, 178–180. [CrossRef] [PubMed]